Essential auditory contrast-sharpening is preneuronal

R. Stoop* and A. Kern

Institute of Neuroinformatics, University/Eidgenössische Technische Hochschule Zürich, Winterthurerstrasse 190, 8057 Zurich, Switzerland

Contrast-sharpening is a fundamental feature of mammalian sensory perception. Whereas visual contrast-sharpening has been fully understood in terms of the retinal neuronal wiring [DeVries, S. H. & Baylor, D. A. (1993) *Cell* 72, Suppl., 139–149], a corresponding explanation of auditory contrast-sharpening is still lacking. Here, we show that the essentials of auditory contrast-sharpening can be explained by using cochlear biophysics. This finding indicates that the phenomenon is basically of preneuronal origin.

Sound impinging on the mammalian ear is transduced into neuronal excitation patterns by means of the cochlea. In 1863, H. L. F. Helmholtz (1) proposed the tonotopic principle to explain the cochlea. According to this principle, there is a mapping between the frequency of an incoming tone and the location of maximal response within the cochlea (termed the characteristic place), analogous to the arrangement of strings on a piano. This linear theory, however, fails to explain important cochlear hearing phenomena, the most prominent being two-tone suppression (2), the principal mechanism underlying auditory contrast-sharpening (3). When two or more tones are presented simultaneously to the cochlea, attenuated responses of the individual tones are evoked, and only the main contributions survive. Understanding the mechanism of two-tone suppression is of both theoretical and practical interest, e.g., for the development of noncontextual measures of hearing loss and the optimization of hearing implants. Here we show that a detailed qualitative and quantitative description of two-tone suppression can be furnished by using a Hopf-type cochlea model.

It is generally assumed that two-tone suppression is based on active hearing processes, i.e., on the ability of the cochlea to selectively amplify its response. Recently, we proposed a biomorphic model of the cochlea that uses subcritical Hopf amplifiers (4) to implement the active processes. For a Hopf system, the steady-state response, R, to a periodic forcing of amplitude, F, and frequency, ω, is determined by a cubic equation in R^2 (5):

$$F^2 = R^6 - 2\mu R^4 + [\mu^2 + (\omega - \omega_0)^2]R^2 . \qquad [1]$$

In Eq. **1**, ω_0 is the frequency at which the optimal response is measured, at a given place. This incorporates the relationship between place and frequency, as given by the tonotopic principle. The control parameter μ measures the distance from the Hopf bifurcation point $\mu = 0$, where the system starts to generate self-oscillations. To describe the amplification of interacting tones, we expanded the response around their noninteracting states and found that their respective active amplifications are also described by Eq. **1**. The presence of two tones of amplitudes, F_t and F_s, however, is now reflected in a pair of *effective* Hopf parameters:

$$\mu_{\mathrm{eff,t}} = \mu - 2R_s^2, \qquad [2]$$

$$\mu_{\mathrm{eff,s}} = \mu - 2R_t^2 .$$

These expressions display the mutual relationship between test F_t and suppressor F_s tones.

In our biomorphic cochlea model, all active contributions $R_{\mathrm{t,s}}$ are locally injected into the passive cochlea, whose behavior is governed by the laws of hydrodynamics. The resulting system can be described by a differential equation for the energy density $e(x, \omega)$, related to the basilar membrane (BM) displacements by

$$A(x, \omega) = \sqrt{\frac{2e(x, \omega)}{E(x)}}, \qquad [3]$$

where $E(x)$ is the exponentially decaying BM stiffness (4). Realistic responses, at biophysical parameter values, are only obtained for $\mu < 0$, i.e., if noncritical tuning is used. A great advantage here is that a single free parameter in the cochlea differential equation suffices to determine the gain and the width of the compressive nonlinear regime. As is shown in Fig. 1, responses obtained from our model closely match physiological measurements of two-tone suppression.

Our approach provides an explanation for the mechanism underlying two-tone suppression. For instance, each curve shown in Fig. 1 indicates that the BM responds with the characteristic Hopf behavior described by Eq. **1**, up to relatively high suppressor intensities. To make this observation more transparent, notice that the BM response $A_{\mathrm{t,s}}$ corresponds to the Hopf response $R_{\mathrm{t,s}}$, whereas the stimulation intensity $I_{\mathrm{t,s}}$ corresponds to the squared forcing $F_{\mathrm{t,s}}^2$. Linear regimes of the test tone input–output function, obtained for weak stimulation, always end up in the compressive nonlinear behavior characteristic of mammalian hearing. This scenario ends in the passive hydrodynamic behavior obtained for very high stimulation intensities. The equivalent situation emerges when a fixed low-intensity test tone is combined with a suppressor of increased intensity, because of the duality between the test and the suppressor tone.

Our biomorphically motivated modeling also allows the quantitative extraction of the scaling in the different regimes of suppressor efficacy, as well as the derivation of the slow onset of suppression. To show this, the correspondence between the cochlea and the Hopf amplifier response needs to be made rigorous, starting from the cochlea differential equation. The detailed analytical derivation of two-tone suppression scaling proceeds along the following lines: Our Hopf cochlea initial value problem has the form (4)

$$\frac{\partial e(x, \omega)}{\partial x} = -\frac{1}{v_{\mathrm{G}}(x, \omega)}\left[\frac{\partial v_{\mathrm{G}}(x, \omega)}{\partial x} + d(x, \omega)\right] e(x, \omega)$$

$$+ \frac{a(x, e(x, \omega), \omega)}{v_{\mathrm{G}}(x, \omega)}, \qquad [4]$$

where d is the dissipation rate, which is counteracted by the power a delivered by the active process. v_{G} is the group velocity. The origin of this equation is in the steady-state energy balance (6) between dissipation and active amplification. The initial energy density $e(x = 0, \omega)$ is derived from the steady-state conditions at the base of the cochlea. There, the rate at which the wave energy exits from the base is equal to the average incoming acoustic power, $P \sim I$ (where I in W·m^{-2} is the sound intensity). From this we obtain

APPLIED PHYSICAL SCIENCES
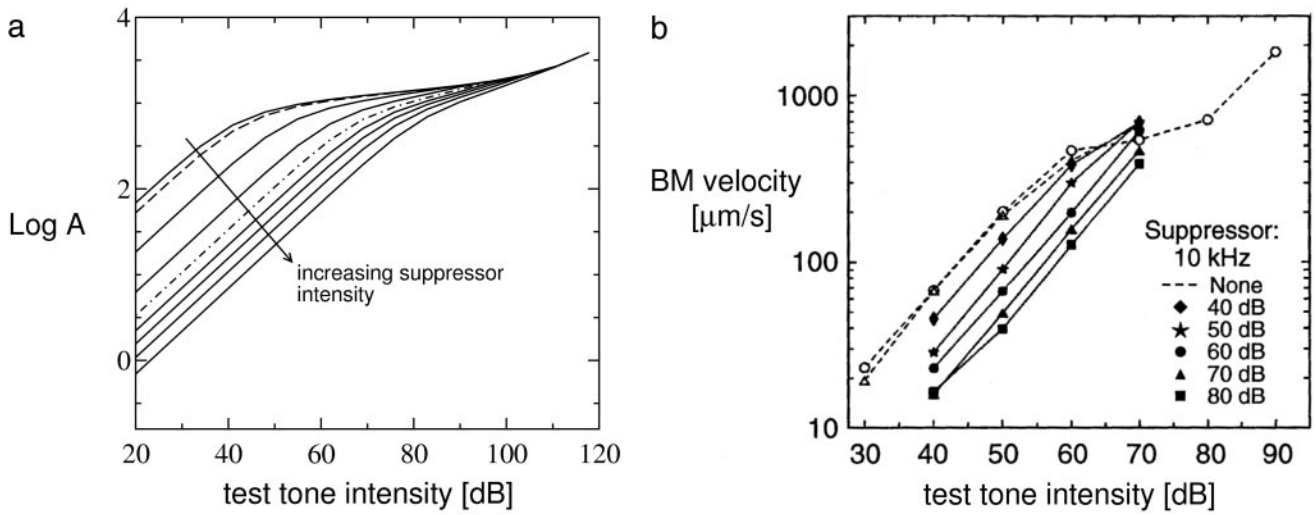
Fig. 1. High-side suppression ($\omega_s > \omega_t$). (*a*) Model response at resonance. Suppressor intensities from 10 to 110 dB, in steps of 10 dB. The 10-, 20-, and 30-dB lines almost coincide. The dashed line separates the onset from the intermediate suppressor regime; the dashed–dotted line separates the intermediate from the compressive-nonlinear suppressor regime ($\omega_t/2\pi = 0.9$ kHz, $\omega_s/2\pi = 1.0$ kHz). (*b*) Laser velocimetry measurements of high-side suppression [chinchilla (3), $\omega_t/2\pi = 8$ kHz]. [*b* is reproduced with permission from ref. 3 (Copyright 1992, Am. Physiol. Soc.).]

$$e(x = 0, \omega) = \frac{P}{\nu_G (x = 0, \omega)} \sim \frac{I}{\nu_G(x = 0, \omega)}. \qquad [5]$$

For a detailed biophysical derivation of the model, where it is also shown how second-order couplings (7) fine-tune the cochlear response shape, see ref. 4.

Because of the mutual role between the test and the suppressor tone, Eq. **2** provides the key mechanism underlying high-side as well as low-side cochlear suppression. This mechanism implies that the discussion of high-side suppression provided below can be applied analogously to low-side suppression. Only the phenomenon of phasic suppression (3, 8), which is of a different (temporal periodic modulation) nature, is not covered in our discussion.

For the derivation of the scaling laws of high-side suppression, we identify the BM-response, $A_{t,s}$, with the Hopf response, $R_{t,s}$, and the stimulation intensity, $I_{t,s}$, with the square of the forcing, $F_{t,s}^2$. In the following discussion, we focus on the linear test-tone regime. There, $I_{t,s} \sim F_{t,s}^2$ always holds, and the identification $A_{t,s} \sim R_{t,s}$ can be made rigorous by referring back to the formal solution of the cochlea equation. For the test tone, $A_t \sim \sqrt{e}$ then corresponds to the response R_t. For weak stimulation F_t, we find

$$R_t \approx \frac{F_t}{\mu_{\text{eff,t}}} = \frac{F_t}{\mu - 2R_s^2}. \qquad [6]$$

The suppression change, Δ_s, caused by increasing the stimulation from a value $F_s(1)$ to $F_s(2)$, is

$$\Delta_s = \log\frac{A_t(F_s(1))}{A_t(F_s(2))} \sim \log\frac{\mu - 2R_s(2)^2}{\mu - 2R_s(1)^2}. \qquad [7]$$

Choosing $F_s(1) = 0$ (no suppressor stimulation), we obtain the onset behavior

$$\Delta_s(\text{ons}) \sim \log\frac{\mu - 2R_s(2)^2}{\mu} \approx \frac{2R_s(2)^2}{\mu}. \qquad [8]$$

For weak stimulations, F_s, we have $R_s^2 \sim F_s^2 \sim I_s$, where I_s is the intensity of suppressor stimulation. This explains the slow departure of the curves from zero suppression. As soon as $R_s^2 \gg \mu$ (intermediate regime), we have

$$\Delta_s(\text{int}) \sim \log\frac{R_s(2)^2}{R_s(1)^2} \approx \log\frac{I_s(2)}{I_s(1)}, \qquad [9]$$

where the last approximation can be justified in the intermediate, suppressor-linear regime only. The result explains the large constant distances between the response curves. When F_s is increased further, the suppressor enters its compressive nonlinear regime. This leads to $R_s^2 \sim F_s^{2/3} \sim I_s^{1/3}$, resulting in

$$\Delta_s(\text{cnl}) \approx \frac{1}{3}\Delta_s(\text{int}). \qquad [10]$$

Thus, the distances between adjacent lines in the compressive nonlinear regime are reduced by a factor of three, compatible with the physiological results. In Fig. 2, the obtained results have been collected, demonstrating the close agreement between suppression derived analytically, simulation results, and physiological measurements.

Results from the nonphasic low-side suppression regime match equally well with the experimental (9) data and further corroborate our approach. Emergent suppression rates, which are larger than those obtained from high-side suppression, can also be fully explained by using arguments parallel to those
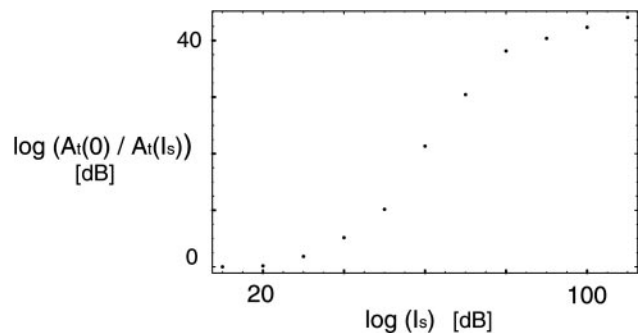
Fig. 2. Typical suppression results obtained from using the estimates of Eqs. 5-7, where the proportionality constants in Eqs. **5** and **6** have been set to unity. The displayed values correspond to the data obtained along the arrow in Fig. 1*a*.

above. To this end, note that the frequency response curve is asymmetrical in shape, with a noncompressive low-frequency tail. In low-side suppression experiments, the difference between test tone and suppressor frequency can be, and usually is, chosen much larger than for the high-side case (e.g., 10 kHz and 500 Hz). Therefore, at the characteristic place of the test tone, the suppressor response R_s will be approximately linear in F_s. The larger suppression growth rates observed in low-side suppression experiments are the immediate consequence of this absence of a compressive nonlinear regime.

We have qualitatively and quantitatively demonstrated that the essentials of two-tone suppression emerge from the interaction between the active elements of the cochlea. Two-tone suppression is considered the main underlying mechanism of auditory signal sharpening (2, 3, 10), although higher, neuronal processing levels also contribute (11). Therefore, our contribution implies that auditory contrast sharpening essentially emerges from cochlear, i.e., preneuronal, Hopf-amplifier biophysics.

The close correspondence between our biomorphically motivated model and the mammalian cochlea can also be used for the detailed simulation of hearing defects, providing a basis for quantitative noncontextual measures of cochlear hearing damage.

1. Helmholtz, H. L. F. (1863) *Die Lehre von den Tonempfindungen als Physiologische Grundlage für die Theorie der Musik* (Vieweg, Braunschweig, Germany).
2. Geisler, C. D. (1998) *From Sound to Synapse: Physiology of the Mammalian Ear* (Oxford Univ. Press, Oxford).
3. Ruggero, M. A., Robles, L. & Rich, N. C. (1992) *J. Neurophysiol.* **68,** 1087–1099.
4. Kern, A. & Stoop, R. (2003) *Phys. Rev. Lett.* **91,** 128101.
5. Eguíluz, V. M., Ospeck, M., Choe, Y., Hudspeth, A. J. & Magnasco, M. O. (2000) *Phys. Rev. Lett.* **84,** 5232–5235.
6. Whitham, G. B. (1999) *Linear and Nonlinear Waves* (Wiley Interscience, New York).
7. Geisler, C. D. & Sang, C. (1995) *Hear. Res.* **86,** 132–146.
8. Cooper, N. P. (1996) *J. Acoust. Soc. Am.* **99,** 3087–3098.
9. Rhode, W. S. & Cooper, N. P. (1996) *Auditory Neurosci.* **3,** 101–121.
10. Moore, B. C. J. (2000) *An Introduction to the Psychology of Hearing* (Academic, London).
11. Sutter, M. L. & Loftus, W. C. (2003) *J. Neurophysiol.* **90,** 2629–2647.

APPLIED PHYSICAL SCIENCES